# Experimental evidence of carrier leakage in InGaAsN quantum-well lasers

Nelson Tansu[a)]
*Center for Optical Technologies, Department of Electrical and Computer Engineering, Lehigh University, Sinclair Laboratory, 7 Asa Drive, Bethlehem, Pennsylvania 18015*

Jeng-Ya Yeh and Luke J. Mawst
*Reed Center for Photonics, Department of Electrical and Computer Engineering, University of Wisconsin-Madison, 1415 Engineering Drive, Madison, Wisconsin 53706*

(Received 12 March 2003; accepted 21 July 2003)

Carrier leakage processes are shown *experimentally* as one of the factors contributing to the temperature sensitivity of InGaAsN quantum well lasers. The utilization of the direct barriers of $GaAs_{0.85}P_{0.15}$ instead of GaAs, surrounding the InGaAsN quantum-well (QW)-active region, leads to significant suppression of carrier leakage at elevated temperatures of 90–100 °C. Threshold current densities of *only* 390 and 440 A/cm$^2$ was achieved for InGaAsN QW lasers ($L_{cav}$ $=2000\ \mu$m) with $GaAs_{0.85}P_{0.15}$-direct barriers at temperature of 80 and 90 °C, respectively. © *2003 American Institute of Physics.* [DOI: 10.1063/1.1611279]

High-performance 1300 nm InGaAsN quantum-well (QW) lasers on a GaAs substrate have been realized by the molecular-beam-epitaxy[1–5] and metalorganic-chemical-vapor-deposition (MOCVD) technologies.[6–11] The early high threshold–current–density ($J_{th}$) InGaAsN QW lasers have demonstrated extremely temperature-insensitive behavior, which has been shown to result from the large monomolecular recombination in the InGaAsN QW active materials.[13] As the material quality and the device performance of InGaAsN QW lasers improved, the $T_0$ values $[1/T_0=1/J_{th}(dJ_{th}/dT)]$ of the lasers were observed to decrease significantly.[6–8,2,11] A decrease in the $J_{th}$ is typically accompanied with a decrease in the $T_0$ values.

There are several possible reasons for the increased temperature sensitivity of the high-performance 1300 nm InGaAsN QW lasers. Recent analysis without taking into consideration any carrier leakage process, has attributed the existence of Auger recombination in InGaAsN QW lasers as the *only* factor that leads to the higher temperature sensitivity found in the high-performance devices.[13] Our previous studies[14] have suggested carrier leakage and a more temperature sensitive material gain are also contributing factors that lead to a stronger temperature sensitivity of the InGaAsN QW lasers in comparison to that of the optimized 1200 nm InGaAs QW lasers.

Here we demonstrate experimental evidence for the existence of temperature-induced carrier leakage in InGaAsN QW lasers. This work shows that carrier leakage in InGaAsN QW cannot be neglected, despite its deep electron confinement. Experiments are designed, in which the choice of the barriers surrounding an identical 60 Å $In_{0.4}Ga_{0.6}As_{0.995}N_{0.005}$ QW ($\Delta a/a\sim 2.8\%$, compressive) are modified from the conventional GaAs barriers to higher band gap ($E_g\sim 1.55$ eV) $GaAs_{0.85}P_{0.15}$ barriers ($\Delta a/a\sim -0.54\%$, tensile), as shown in Figs. 1 and 2. By replacing the direct barrier material, the thermionic escape lifetime of the carriers in the QW will be altered as a consequence of changes in the band offsets ($\Delta E_b$). By utilizing the GaAsP-direct barriers, significant suppression of the carrier leakage phenomena at elevated temperature is observed, resulting in the realization of InGaAsN–QW lasers with low $J_{th}$ and improved $T_0$ values at elevated temperatures. It is also important to note that the improvement in $T_0$ values in the InGaAsN–GaAsP laser structure is not a result of an increase in the $J_{th}$.

The $J_{th}$ of QW lasers can be expressed as a function of device parameters, which include transparency current density ($J_{tr}$), current injection efficiency ($\eta_{inj}$), material gain parameter ($g_{0j}$), and internal loss ($\alpha_i$), as follows:[12]

$$J_{th}=\frac{J_{tr}}{\eta_{inj}}\cdot\exp\left(\frac{\alpha+(1/L)\ln(1/R)}{\Gamma g_{0J}}\right). \tag{1}$$

The $\eta_{inj}$ is defined as the fraction of the injected current that recombines in the QW active region. An expression for $\eta_{inj}$ at threshold,[15,16] with the assumption of low photon density ($S$), can be expressed as follows:

$$\eta_{inj}(S\to 0)\cong\frac{1}{1+\frac{\tau_{bw}}{\tau_b}\cdot\left(1+\frac{\tau_{QW_total}}{\tau_e}\right)}, \tag{2}$$

with $\tau_{bw}$ as the total carrier transport time, $\tau_b$ as the total recombination lifetime in the separate-confinement-heterostructure (SCH) region, $\tau_{QW_total}$ as the total recombination lifetime in the QW active region, and $\tau_e$ as the thermionic carrier escape lifetime. The expression in Eq. (2) can be derived from the conventional rate equation for QW lasers.[15,16] The $\tau_{bw}$ and $\tau_b$ are assumed as unchanged in all our experiments, as the design and the choice of material systems of the SCH region are identical for all structures investigated here. From the fact that the compositions and dimensions of the InGaAsN QW active regions in both experiments are kept identical, the total recombination lifetime in QW $\tau_{QW_total}$ can also be assumed as unchanged.

The thermionic escape lifetime ($\tau_{e_e,h}$ for electrons and holes, respectively) of the carriers in the QW can be expressed as follows[15,17,18]

[a)]Electronic mail: tansu@lehigh.edu

 © 2003 American Institute of Physics
Downloaded 20 Jul 2011 to 128.180.137.141. Redistribution subject to AIP license or copyright; see http://apl.aip.org/about/rights_and_permissions

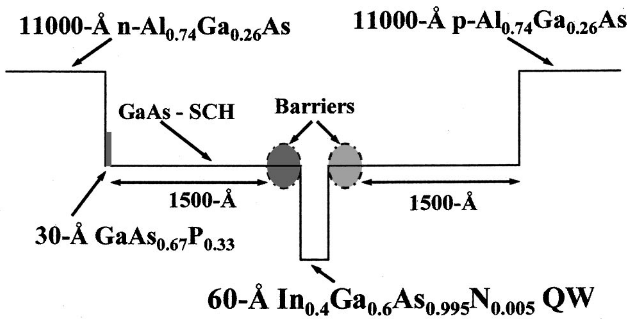


FIG. 1. Cross-sectional schematic band diagram of InGaAsN QW lasers.

$$\frac{1}{\tau_{e_e,h}} \propto \frac{1}{N_{\mathrm{QW}} \cdot L_z} \cdot T^2 \cdot \exp\left(-\frac{\Delta E_{b_e,h}}{k_B \cdot T}\right), \tag{3}$$

with $k_B$ as the Boltzmann constant, $T$ as the temperature, $N_{\mathrm{QW}}$ as the carrier density in QW, $L_z$ as the thickness of QW, and $\Delta E_{b_e,h}$ as the carrier confinement energy in QW (for electrons and holes, respectively). As the dimension ($L_z$) and composition of the InGaAsN QW active regions in both experiments are identical, the threshold carrier density in the QW ($N_{\mathrm{QW_th}}$) can also be assumed as identical for both lasers with similar confinement and cladding layer designs. The total thermionic carrier escape time of QW ($\tau_e$) can be expressed as functions of the $\tau_{e_\mathrm{electron}}$ and $\tau_{e_\mathrm{holes}}$ as $1/\tau_e = 1/\tau_{e_\mathrm{electron}} + 1/\tau_{e_\mathrm{holes}}$. The escape phenomenon is dominated by the escape rate of the carriers with the fastest escape time. Once the carriers escape, the carriers in the QW and SCH will redistribute themselves to maintain charge neutrality in the QW and SCH due to the high mobility of the carriers.[16] The differences in the $\tau_e$ of InGaAsN–GaAs and InGaAsN–GaAsP structures can be attributed solely to the differences in their respective ratios of $\Delta E_{b_e,h}/k_B T$. The ratios of the electron and hole confinement energy ($\Delta E_c : \Delta E_v$, with $\Delta E_c = \Delta E_{b_e}$, $\Delta E_v = \Delta E_{b_h}$) in InGaAsN–GaAs structures is approximately 80:20,[18,19] resulting in extremely strong electron confinement and extremely poor heavy hole confinement. The calculated escape lifetime of the electrons and holes from InGaAsN QW is approximately 30–50 ns and 5–10 ps, respectively, for near-threshold conditions.[18] By utilizing the large bandgap material surrounding the InGaAsN QW, the confinement energy of both the electrons and holes in the QW will be increased.

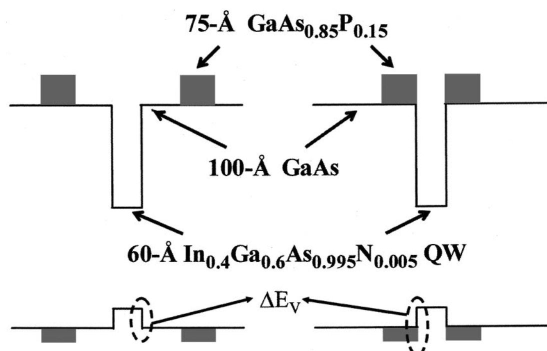


FIG. 2. Schematic band diagram of the $In_{0.4}Ga_{0.6}As_{0.995}N_{0.005}$ QW active regions with direct barriers of (a) GaAs and (b) $GaAs_{0.85}P_{0.15}$.

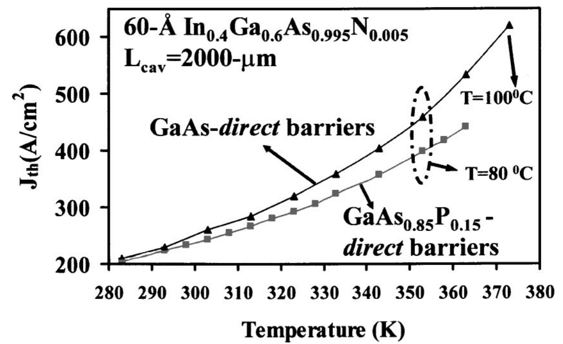


FIG. 3. The measured threshold current densities of InGaAsN–GaAs QW and InGaAsN–GaAsP QW lasers as function of temperature, for as-cleaved with $L_{\mathrm{cav}} = 2000\ \mu$m.

As no studies have been reported on the InGaAsN–GaAsP structures, the $\Delta E_c : \Delta E_v$ ratio is assumed as similar with that of InGaAsN–GaAs case. The calculated increase in $\Delta E_v$ (without taking into account the tensile strain of GaAsP) of approximately 22–35 meV can be achieved for the InGaAsN–GaAsP structures, which is approximately 25% larger than that of InGaAsN–GaAs structures ($\Delta E_v \sim 99$ meV, Ref. 18). Slight increase in $\Delta E_v$ leads to significant suppression of hole escape rate ($1/\tau_e$) from the InGaAsN–GaAsP QW structures due to its exponential relation [from Eq. (3)], which will in turn lead to improved $\eta_{\mathrm{inj}}$ and $J_{\mathrm{th}}$ at elevated temperatures [from Eqs. (1) and (2)]. In the absence of any carrier leakage, by contrast, an increase in $\Delta E_v$ will not lead to any reduction in $J_{\mathrm{th}}$ at elevated temperatures or any improvement in the $T_0$ values. The tensile strain of GaAsP barriers could potentially lead to even further improved confinement of heavy holes in InGaAsN QW, due to the strain-induced lowering of the heavy-hole band edge of tensile strain material.

Both laser structures studied here, shown in Figs. 1 and 2, were grown by low-pressure MOCVD. The group-V precursors are arsine ($AsH_3$) and phosphine ($PH_3$). The group-III precursors are the trimethyl (TM) sources of Ga, Al, and In. The N-precursor is U-dimethylhydrazine (U-DMHy). The dopant sources are $SiH_4$ and dielthylzinc (DEZn) for the $n$ and $p$ dopants, respectively. The detail of the MOCVD growth of InGaAsN QW materials utilizing GaAs barriers and larger band gap materials of GaAsP has been discussed elsewhere in Refs. 6, 7, and 20.

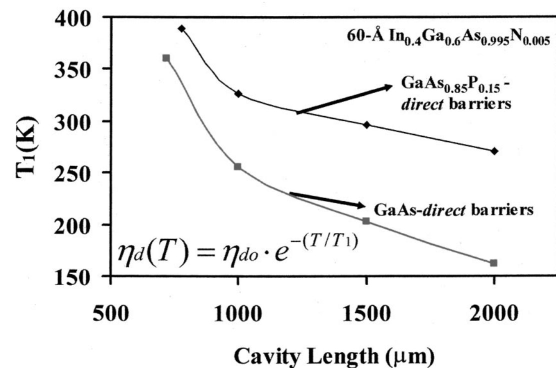


FIG. 4. The comparison of $T_1$ values, measured from temperature of 10 to 60 °C, for $In_{0.4}Ga_{0.6}As_{0.995}N_{0.005}$ QW lasers with $GaAs_{0.85}P_{0.15}$ barriers and GaAs barriers, for various cavity lengths.

Downloaded 20 Jul 2011 to 128.180.137.141. Redistribution subject to AIP license or copyright; see http://apl.aip.org/about/rights_and_permissions

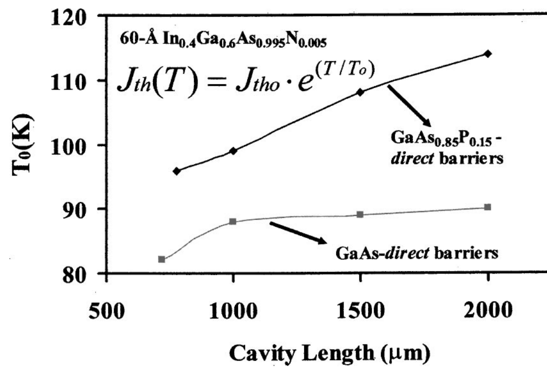


FIG. 5. The comparison of $T_0$ values, measured from temperature of 10 to 60 °C, for $In_{0.4}Ga_{0.6}As_{0.995}N_{0.005}$ QW lasers with $GaAs_{0.85}P_{0.15}$ barriers and GaAs barriers, for various cavity lengths.

As-cleaved broad area lasers, with oxide-defined stripe width of 100 $\mu$m, were fabricated for both active regions shown in Fig. 2. The lasing characteristics were measured under pulsed conditions with a pulse width and a duty cycle of 5 $\mu$s and 1%, respectively. Room-temperature threshold current densities of 320, 260, and 220 A/cm$^2$ were measured for InGaAsN–GaAsP QW lasers for cavity lengths of 775, 1000, and 2000 $\mu$m, respectively. At room temperature ($T = 20\,°$C), threshold characteristics of both the InGaAsN–GaAs are measured as approximately 350–360, 250, and 210–220 A/cm$^2$, for devices with cavity lengths of 720, 1000, and 2000 $\mu$m, respectively. The emission wavelength of the InGaAsN–GaAsP lasers is approximately 1280 nm ($L_{cav} = 2000\,\mu$m), which is approximately 150 Å shorter than that of the InGaAsN–GaAs QW structures. Calculations considering the band gap, strain, and effective masses predict a blueshift of the emission wavelength of approximately 100–120 Å for InGaAsN–GaAsP QW structures, in good agreement with experiments.

The temperature characterizations of both InGaAsN–GaAsP and InGaAsN–GaAs QWs lasers are performed over the range of 10–100 °C. The characteristics of $J_{th}$ with temperatures for both laser structures ($L_{cav} = 2000\,\mu$m) are plotted in Fig. 3. The measurement is conducted for devices with long cavity to minimize the effect from the temperature sensitivity of material gain.[12] Threshold current densities of both lasers are nearly identical in the temperature regime below 20 °C. As the temperature increases, the $J_{th}$ of the InGaAsN with GaAsP barriers increases at a significantly slower rate. The suppression of carrier leakage is also evident from the fact that the $T_0$ and $T_1$ ($1/T_1 = -(1/\eta_d) d\eta_d/dT$, $\eta_d$ = external differential quantum efficiency) values of the InGaAsN–GaAsP structures are significantly improved for devices with various cavity lengths, as shown in Figs. 4 and 5. Threshold current densities of only 390 and 440 A/cm$^2$ were also measured for InGaAsN–GaAsP QW lasers ($L_{cav} = 2000\,\mu$m) at temperatures of 80 and 90 °C, respectively. As electrons are very well confined in both InGaAsN QW laser structures, the reduction of the $J_{th}$ of the InGaAsN–GaAsP QW structures at elevated temperatures as well as their improved $T_0$ and $T_1$ values are results of suppression of heavy hole leakage from the InGaAsN QW due to the lower hole escape rate ($1/\tau_{e_hole}$).

In summary, the existence of carrier leakage in InGaAsN QW lasers has been demonstrated experimentally as one of the contributing factors influencing the temperature sensitivity of InGaAsN lasers. It is important to note that while these experiments demonstrate the existence of a carrier leakage processes in InGaAsN QW lasers, they do not rule out Auger recombination as an additional contributing factor for the device temperature sensitivity. Suppression of carrier leakage in InGaAsN QW lasers with larger band gap barrier material of GaAsP leads to a reduction in the $J_{th}$ at elevated temperature, accompanied by the increase in the $T_0$ and $T_1$ values. The $J_{th}$ of the InGaAsN QW lasers ($L_{cav} = 2000\,\mu$m, as-cleaved), with $GaAs_{0.85}P_{0.15}$-direct barriers, have been measured as *only* 220 and 390 A/cm$^2$, for measurements at temperature of 20 and 80 °C, respectively.

[1] D. A. Livshits, A. Yu. Egorov, and H. Riechert, Electron. Lett. **36**, 1381 (2000).
[2] W. Ha, V. Gambin, M. Wistey, S. Bank, S. Kim, and J. S. Harris, Jr., IEEE Photonics Technol. Lett. **14**, 591 (2002).
[3] C. S. Peng, T. Jouhti, P. Laukkanen, E.-M. Pavelescu, J. Konttinen, W. Li, and M. Pessa, IEEE Photonics Technol. Lett. **14**, 275 (2002).
[4] J. Wei, F. Xia, C. Li, and S. R. Forrest, IEEE Photonics Technol. Lett. **14**, 597 (2002).
[5] K. D. Choquette, J. F. Klem, A. J. Fischer, O. Blum, A. A. Allerman, I. J. Fritz, S. R. Kurtz, W. G. Breiland, R. Sieg, K. M. Geib, J. W. Scott, and R. L. Naone, Electron. Lett. **36**, 1388 (2000).
[6] N. Tansu and L. J. Mawst, IEEE Photonics Technol. Lett. **14**, 444 (2002).
[7] N. Tansu, N. J. Kirsch, and L. J. Mawst, Appl. Phys. Lett. **81**, 2523 (2002).
[8] N. Tansu, A. Quandt, M. Kanskar, W. Mulhearn, and L. J. Mawst, Appl. Phys. Lett. **83**, 18 (2003).
[9] T. Takeuchi, Y.-L. Chang, M. Leary, A. Tandon, H.-C. Luan, D. P. Bour, S. W. Corzine, R. Twist, and M. R. Tan, IEEE LEOS 2001 Post-Deadline Session, 2001.
[10] M. Kawaguchi, T. Miyamoto, E. Gouardes, D. Schlenker, T. Kondo, F. Koyama, and K. Iga, Jpn. J. Appl. Phys., Part 2 **40**, L744 (2001).
[11] N. Tansu and L. J. Mawst, IEEE Photonics Technol. Lett. **13**, 179 (2001).
[12] N. Tansu, Y. L. Chang, T. Takeuchi, D. P. Bour, S. W. Corzine, M. R. T. Tan, and L. J. Mawst, IEEE J. Quantum Electron. **38**, 640 (2002).
[13] R. Fehse, S. Tomic, A. R. Adams, S. J. Sweeney, E. P. O'Reilly, A. Andreev, and H. Riechert, IEEE J. Sel. Top. Quantum Electron. **8**, 801 (2002).
[14] N. Tansu and L. J. Mawst, IEEE Photonics Technol. Lett. **14**, 1052 (2002).
[15] N. Tansu and L. J. Mawst (unpublished).
[16] R. Nagarajan and J. E. Bowers, IEEE J. Quantum Electron. **29**, 1601 (1993).
[17] M. Irikawa, T. Ishikawa, T. Fukushima, H. Shimizu, A. Kasukawa, and K. Iga, Jpn. J. Appl. Phys., Part 1 **39**, 1730 (2000).
[18] N. Tansu and L. J. Mawst, Appl. Phys. Lett. **82**, 1500 (2003).
[19] M. Hetterich, M. D. Dawson, A. Yu. Egorov, D. Bernklau, and H. Riechert, Appl. Phys. Lett. **76**, 1030 (2000).
[20] N. Tansu, J. Y. Yeh, and L. J. Mawst, Appl. Phys. Lett. **82**, 3008 (2003).

Downloaded 20 Jul 2011 to 128.180.137.141. Redistribution subject to AIP license or copyright; see http://apl.aip.org/about/rights_and_permissions